Novel Multifunctional Nanomatrix Reduces Inflammation in Dynamic Conditions in Vitro and Dilates Arteries ex Vivo

Grant C. Alexander,[†] Jeremy B. Vines,[†] Patrick Hwang,[†] Teayoun Kim,[‡] Jeong-a Kim,[‡] Brigitta C. Brott,[§] Young-Sup Yoon,[⊥,∥] and Ho-Wook Jun*,[†]

[†]Department of Biomedical Engineering, [‡]Department of Medicine, Division of Endocrinology, Diabetes and Metabolism, and [§]School of Medicine, Division of Cardiology, University of Alabama at Birmingham, 806 Shelby Building, 1825 University Boulevard, Birmingham, Alabama 35294, United States
[⊥]School of Medicine, Division of Cardiology, Emory University, Atlanta, Georgia 30322, United States
[∥]Severance Biomedical Science Institute, Yonsei University College of Medicine, Seoul, Korea

ABSTRACT: Inflammatory responses play a critical role in tissue−implant interactions, often limiting current implant utility. This is particularly true for cardiovascular devices. Existing stent technology does little to avoid or mitigate inflammation or to influence the vasomotion of the artery after implantation. We have developed a novel endothelium-mimicking nanomatrix composed of peptide amphiphiles that enhances endothelialization while decreasing both smooth muscle cell proliferation and platelet adhesion. Here, we evaluated whether the nanomatrix could prevent inflammatory responses under static and physiological

flow conditions. We found that the nanomatrix reduced monocyte adhesion to endothelial cells and expression of monocyte inflammatory genes (TNF-α, MCP-1, IL-1β, and IL-6). Furthermore, the nitric-oxide releasing nanomatrix dramatically attenuated TNF-α-stimulated inflammatory responses as demonstrated by significantly reduced monocyte adhesion and inflammatory gene expression in both static and physiological flow conditions. These effects were abolished by addition of a nitric oxide scavenger. Finally, the nanomatrix stimulated vasodilation in intact rat mesenteric arterioles after constriction with phenylephrine, demonstrating the bioavailability and bioactivity of the nanomatrix, as well as exhibiting highly desired release kinetics. These results demonstrate the clinical potential of this nanomatrix by both preventing inflammatory responses and promoting vasodilation, critical improvements in stent and cardiovascular device technology.

KEYWORDS: inflammation, nanomatrix, endothelium, vasodilation, bioreactor, stent
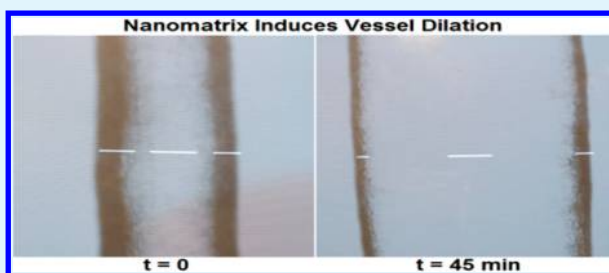
1. INTRODUCTION

It is well-known that inflammation is a major factor in many, if not all, diseases, including cardiovascular disease (CVD). Atherosclerosis—the hardening of the artery lumen, and a major underlying factor in CVD − is mediated to a great extent by vascular inflammation, which has already been characterized in detail.[1] Briefly, injury or insult to the vascular endothelial lumen results in increased attraction and attachment of circulating monocytes, neutrophils, and T lymphocytes. After subendothelium localization, the monocytes differentiate into macrophages, which ingest lipoproteins and become foam cells. These foam cells accumulate along with the other immune cells to form fatty streaks or plaques, which may damage the endothelium, leading to smooth muscle cells proliferation, neointimal hyperplasia, thrombosis, and occlusion of the blood vessel.[1,2]

Many molecular mediators are known to regulate the inflammatory process. For example, tumor necrosis factor-alpha (TNF-α), interleukin-1β (IL-1β), and interleukin-6 (IL-6), among other cytokines, have been demonstrated to induce and direct pro-inflammatory responses within the vasculature

along with chemotactic agents such as monocyte chemo-attractant protein-1 (MCP-1).[1,3−6] Particularly for arteries and CVD, TNF-α acts in a potent multifaceted fashion via the following pathways: upregulation of smooth muscle cell proliferation, leading to neointimal hyperplasia and restenosis; modulation of inflammatory responses after lumen injury, resulting in endothelial cell dysfunction through impairment of nitric oxide synthesis and upregulation of adhesion molecules for monocyte binding; and recruitment and activation of inflammatory cells such as macrophages and monocytes.[1,3] In light of the significant role that inflammation plays in CVD, controlling the inflammatory response is a key consideration in biocompatible cardiovascular implant development, particularly in the context of a pre-existing inflammatory environment such as occurs with CVD.

Stents are widely used in CVD treatment. The initial bare-metal stent design resulted in unacceptable levels of restenosis;
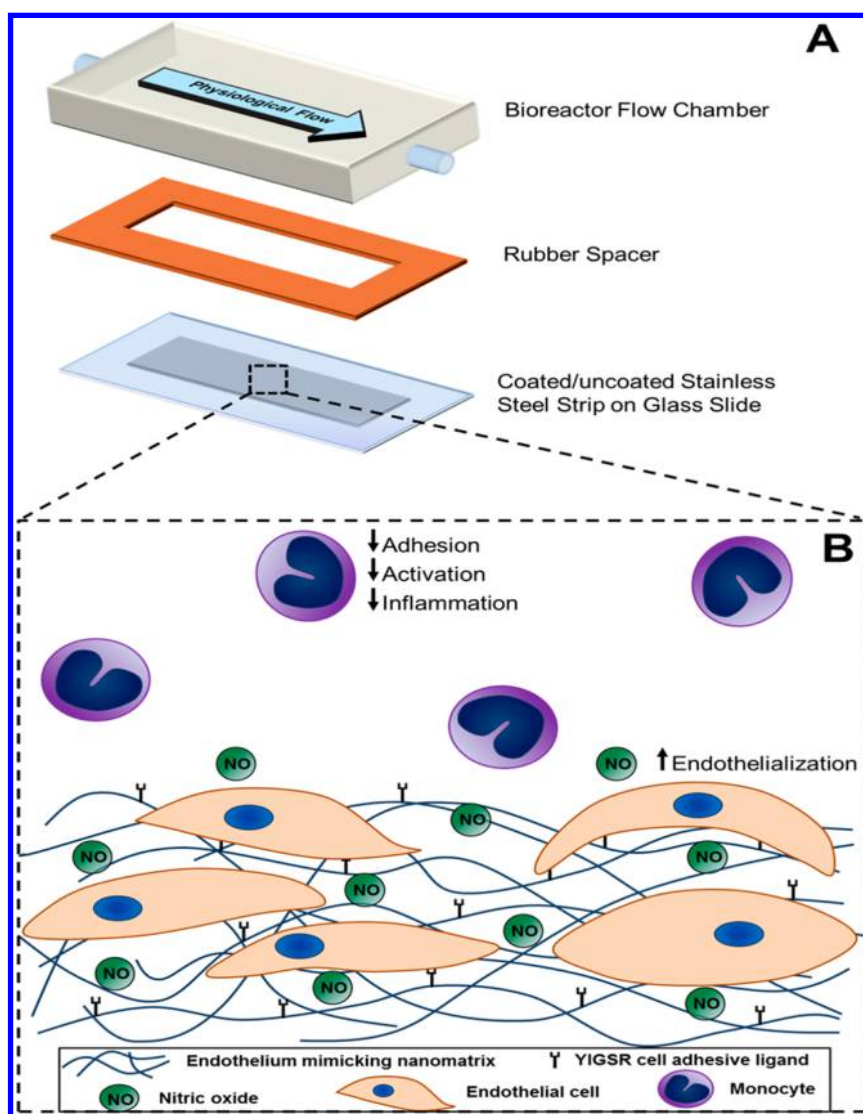
Figure 1. (A) Physiological-condition modeling bioreactor setup schematic. (B) Endothelium mimicking nanomatrix, composed of YIGSR endothelial cell adhesive ligands, MMP-2 enzyme-mediated degradable sequences, and polylysine NO-donating residues, increases endothelialization while simultaneously decreasing inflammatory responses.

to address this problem, drug-eluting stents (DES) were developed to reduce neointimal hyperplasia and thus preserve vessel patency. However, the shortcomings of DES have become apparent; in particular, belated endothelial lumen healing and late stent thrombosis have led to questions over DES efficacy.[7−10] Moreover, investigators have found adverse inflammatory responses to DES, detecting elevated levels of IL-1, IL-6, and other pro-inflammatory cytokines, which can persist for months.[9,11−17] Additional inflammatory responses may arise due to the antiplatelet regimens, such as clopidogrel, that may be necessary after DES deployment.[18,19] This kind of chronic inflammation impedes vessel lumen healing, thus contributing significantly to late stent thrombosis.[1,20] These studies highlight the importance of stent coatings that are biocompatible while simultaneously circumventing the shortcomings of restenosis, thrombosis, neointimal hyperplasia, and inflammation.

To this end, we have developed an innovative endothelium-mimicking nanomatrix composed of peptide amphiphiles (PAs) that self-assemble into nanofibers through a water evaporation technique without the use of potentially inflammatory organic solvents.[16,21] These PAs incorporate enzyme-mediated degradable sites for remodeling, laminin-derived cell adhesive ligands for endothelial cell attachment, and polylysine nitric oxide donors in optimized ratios for a vessel healing strategy.[22,23] The optimized cell adhesive ligand-containing and nitric oxide-releasing PAs (PA-YK-NO) self-assemble into nanofibers, forming the endothelium-mimicking nanomatrix. Our previous studies have shown that the nanomatrix enhances endothelialization while decreasing both smooth muscle cell proliferation and platelet adhesion in vitro.[22,23] The nanomatrix also enhances endothelial progenitor cell adhesion and differentiation; furthermore, the nanomatrix coating is stable under physiological flow rates.[24,25] In light of these desired properties and the significant concerns of inflammatory responses to biomedical devices, it is also imperative to evaluate whether and to what extent the nanomatrix coating elicits an inflammatory response that could undermine the clinical utility of the stent coating.

This current work focuses on evaluation of inflammation on the nanomatrix coating in vitro and the coating's vasodilatory effects ex vivo. The incorporation of endothelial cell adhesive

ligands, enzyme-mediated degradable sequences, and nitric oxide (NO)-donating residues can increase endothelialization while simultaneously decreasing inflammatory responses (Figure 1B), resulting in an innovative, multifunctional approach to stent coating design and vessel healing. Employing adhesion assays and quantitative RT-PCR analysis of U937 monocytes under both static and dynamic conditions, we investigated inflammatory effects of our nanomatrix coating for stents. Because NO is known to mitigate inflammation, we then expanded the study beyond inflammatory induction analysis and investigated whether the nanomatrix coating could attenuate a pre-existing inflammatory environment induced by TNF-α.[26−28] Finally, we evaluated the bioavailability and bioactivity of the nanomatrix coating in intact rat mesenteric arterioles through a vasodilation experiment, demonstrating the ability of the NO-releasing nanomatrix coating to successfully dilate phenylephrine-constricted arterioles. In addition to our previous data, these studies are important to ensure that the nanomatrix coating does not cause an inflammatory response and to evaluate whether it can reduce inflammation, a key consideration in stent coatings.

2. MATERIALS AND METHODS

2.1. Preparation of the Self-Assembled Nanomatrix. The nanomatrix was synthesized as previously described.[22−25] Briefly, two different PAs were synthesized through Fluorenylmethoxycarbonyl (Fmoc) chemistry. The first PA was composed of an endothelial cell adhesive ligand (YIGSR) coupled with a matrix metalloprotease-2 (MMP-2) degradable sequence (GTAGLIGQ) to form PA-YIGSR. The second PA contained a nitric oxide (NO) donor polylysine (KKKKK) linked to the MMP-2 degradable sequence, forming PA-KKKKK. The two PAs were mixed in a 9:1 ratio to form PA-YK as previously described and reacted with NO to form PA-YK-NO, the endothelium-mimicking nanomatrix. Self-assembly of PA-YK and PA-YK-NO was achieved by a water evaporation method.[22−25]

2.2. Static Monocyte Adhesion Assay. Two hundred microliters of solution (PA-YK-NO, PA-YK, or deionized (DI) water control) was added to a 48-well tissue culture plate (TCP) and allowed to self-assemble into nanomatrix coatings as previously described.[22,23] After drying, the treated wells were washed with DI water and UV sterilized for 2 h. Human umbilical vein endothelial cells (HUVECs) were seeded at 15 000 cells/cm^2. After 20 h of culture, HUVECs were incubated with or without TNF-α (10 ng/mL) for 4 h to stimulate inflammatory conditions. The HUVECs were then washed twice with warm, sterile PBS. U937 monocytes labeled with CellTracker Green CMFDA (Life Technologies) were then seeded on the HUVECs at a monocyte/endothelial cell ratio of 6:1. After 4 h, unbound cells and media were aspirated from each well for unbound fraction determination. HUVECs were washed twice with warm sterile phosphate buffered saline (PBS) to remove loosely bound monocytes. Monocyte adhesion was analyzed using Nikon NIS Elements imaging software (Melville, NY) and a BioTek Synergy H1 microplate reader (BioTek Instruments, Inc.) at excitation and emission wavelengths of 485 and 528 nm, respectively.

2.3. Quantitative RT-PCR. Coatings were prepared as described and incubated with U937 monocytes (1 × 10^6 cells/mL) with or without TNF-α (10 ng/mL) for 4 or 24 h. Total RNA was isolated using Trizol (Life Technologies) according to the manufacturer's protocol and quantified with a BioTek Synergy H1 microplate reader (BioTek Instruments, Inc.). cDNA was synthesized using a Verso cDNA Kit (Thermo Fisher Scientific) according to the manufacturer's protocol. Forward and reverse primers, respectively, were designed with Primer3[41] for TNF-α (ATGTGGCAAGAGATGGGGAA and CTCACACCCCACATCTGTCT), MCP-1 (GCAGCAAGTGTCC-CAAAGAA and AGGTGGAGAGTGATGTTG GG), IL-1β (GGCTTCCTTCCTTCCTTCCT and CAGT-GAGGTTCCTTGGCCTA), IL-6 (GAAAGGAGGTGGG-

TAGGCTT and AGGTGGGCATGGATTTCAGA), and 18S (AGAAACGGCTACCACATCCA and CCCTCCAATG-GATCCTCGTT). mRNA expression was analyzed via quantitative RT-PCR using ABsolute Blue qPCR SYBR Green master mix (Thermo Fisher Scientific) and a LightCycler 480 (Roche). Fold changes in expression were calculated utilizing the $\Delta\Delta C_T$ method compared with 18S and control expression.

2.4. Rotational Coating Method. Coating of PA-YK and PA-YK-NO via water-evaporation based self-assembly was achieved by a rotational coating technique as previously described.[25] Briefly, the substrate mounted on a rotating mandrel attached to a motor was immersed within PA-YK or PA-YK-NO solution contained in an open top reservoir for 12 h. The rotation ensured uniform coating of the nanomatrix on all substrate surfaces, while the open top of the reservoir facilitated evaporation. After immersion in PA-YK or PA-YK-NO solution for 12 h, the substrate was allowed to dry for 24 h. Substrates were then washed twice with sterile DI water and UV sterilized for 2 h.

2.5. Bioreactor Design. The bioreactor was set up as previously described and is shown in Figure 1A.[25,29] Stainless steel strips (1 cm × 3 cm), chosen as the model stent material, were coated with PA-YK, PA-YK-NO, or left uncoated, and placed within the parallel plate flow chamber. The flow chamber was connected to a media reservoir and a peristaltic pump, which perfused cell culture media at 10 dyn/cm^2. The flow rate was determined based on physiological shear stress, which ranges from 5 to 10 dyn/cm^2 for arteries.[30,31]

2.6. Dynamic Monocyte Adhesion and Quantitative RT-PCR Assays. Stainless steel strips (1 cm × 3 cm) were coated with PA-YK, PA-YK-NO, or left uncoated as described above. HUVECs were seeded on the strips at 15,000 cells/cm^2. After 20 h of culture, HUVECs were incubated with or without TNF-α (10 ng/mL) for 4 h to stimulate inflammatory conditions. The HUVECs were then washed twice with warm, sterile PBS. U937 monocytes (1 × 10^6 cells/mL) labeled with CellTracker Green CMFDA (Life Technologies) were then seeded in the bioreactor and perfused over the HUVEC-covered stainless steel strips at 10 dyn/cm^2 with or without 100 μM carboxy-PTIO (2-(4-carboxyphenyl)-4,4,5,5-tetramethylimidazoline-1-oxyl-3-oxide potassium salt; Sigma), a NO scavenger. After 4 h, stainless steel strips were removed from the bioreactor and washed twice with warm sterile PBS to remove loosely bound monocytes. Monocyte adhesion was analyzed using Nikon NIS Elements imaging software (Melville, NY). For quantitative RT-PCR, stainless steel strips were coated as described and U937 monocytes (1 × 10^6 cells/mL) with or without TNF-α (10 ng/mL) and with or without carboxy-PTIO (100 μM) were perfused over them for 4 or 24 h at 10 dyn/cm^2. RNA isolation, cDNA synthesis, and PCR were performed as described above.

2.7. Immunocytochemistry. Stainless steel strips (1 cm × 3 cm) were coated with PA-YK or PA-YK-NO as described above. GFP-transfected HUVECs (for NF-κB) or regular HUVECs (for VCAM-1) were seeded on the strips at 15,000 cells/cm^2. After 1 day of culture, HUVEC seeded strips were placed in the bioreactor; media with or without TNF-α (10 ng/mL) was then perfused over them for 4 h at 10 dyn/cm^2. After 4 h, the strips were removed from the bioreactor and washed with PBS. Cells were then fixed in 4% paraformaldehyde-PBS for 10 min and then washed twice with PBS for 5 min. For NF-κB only, cells were then permeabilized with 0.1% Triton-X-100-PBS for 5 min and then washed twice with PBS for 5 min. Cells were then blocked with 3% BSA-PBS for 40 min, then incubated with the primary antibody in 3% BSA-PBS at 4 °C overnight (Pierce anti-NF-κB p65, Pierce anti-VCAM-1/CD106; Thermo Scientific). Cells were then washed three times with PBS for 5 min, incubated with Alexa Fluor 555 goat antirabbit IgG (H+L) (Life Technologies) in 3% BSA-PBS at room temperature in the dark for 1 h, washed three times with PBS in the dark for 5 min, stained with 4′,6-Diamidino-2-Phenyl-indole, Dihydrochloride (DAPI) for 10 min in the dark, and examined with a fluorescent microscope at 40× magnification using Nikon NIS Elements imaging software (Melville, NY).

2.8. Ex Vivo Vasodilation in Rat Mesenteric Arterioles. A mesenteric arteriole vasodilation experiment was done as previously
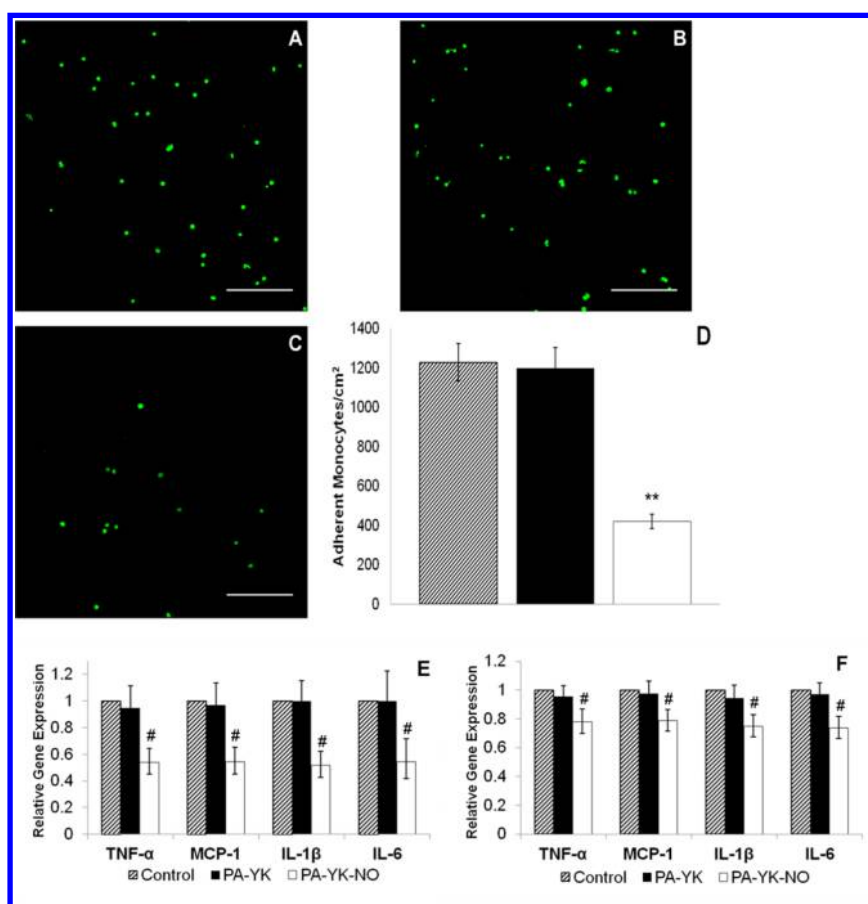
Figure 2. Static monocyte adhesion on HUVECs on (A) TCP control, (B) PA-YK, and (C) PA-YK-NO at 4 h. Scale bar = 300 μm. (D) Adherent monocyte quantification on TCP Control, PA-YK, and PA-YK-NO at 4 h. (E, F) Relative gene expression of monocytes at (E) 4 and (F) 24 h. Bars show mean ± standard deviation. #$p < 0.05$. **$p < 0.001$.

described and is shown in Figure 7A.[32] Male Sprague−Dawley rats (280−300 g) were anesthetized with an intraperitoneal injection of pentobarbital sodium (100 mg/kg). Mesenteric arterioles were excised from the animal and placed in a cooled (4 °C) chamber containing dissection buffer. The isolated arterioles were then cannulated with glass micropipettes with monofilament suture and mounted in a custom-designed tissue chamber as depicted in Figure 7B (Living System Instrumentation, Burlington, VT). The arterioles were pressurized to 100 mmHg intraluminally with the same buffer without flow. After baseline diameter was established, vessels were treated with the vasoconstrictor phenylephrine (10^{-6} M) until maximal, stable constriction was observed. PA-YK-NO and PA-YK coatings were prepared on 12 mm glass coverslips as previously described and incubated with the vessels.[22] PA-YK-NO and PA-YK solutions were also prepared as described and incubated with the vessels to compare release kinetics. Vessel diameter change during the dilation response was recorded by Lab Chart software (AD Instruments, Colorado Springs, CO).

2.9. Statistical Analysis. All experiments were performed at least 3 times with at least 4 replicates per experiment. All values are expressed as mean ± standard deviation. Statistical analysis was performed using one-way ANOVA with Tukey post-test using SPSS software with $p < 0.05$ considered significant.

3. RESULTS AND DISCUSSION

3.1. Peptide Amphiphile Nanomatrix. The PA nanomatrix was successfully synthesized, mixed in a 9:1 ratio, reacted with NO gas, and allowed to self-assemble via the water evaporation method as previously described.[22−25]

3.2. Nanomatrix Does Not Elicit an Inflammatory Response under Static Conditions. Inflammation is a major contributor to vascular neointimal hyperplasia and the resultant restenosis and failure of currently available stents.[9,11−17] Thus, we first sought to determine if and to what extent our PA nanomatrix induced inflammation. Figure 2 shows monocyte adhesion on HUVECs cultured on tissue culture plate (TCP), PA-YK, and PA-YK-NO. Monocyte adhesion was significantly decreased on HUVECs cultured on PA-YK-NO (420 ± 36 cells/cm²) compared to both TCP (1229 ± 95 cells/cm²) and PA-YK (1199 ± 104 cells/cm²) controls ($p < 0.001$) as shown from both image (Figure 2A-C) and cell count (Figure 2D) data, while adhesion counts between TCP and PA-YK were comparable. This was further validated through qRT-PCR analysis of monocyte inflammatory gene expression. PA-YK-NO significantly decreased the four inflammatory genes TNF-α, MCP-1, IL-1β, and IL-6 compared to both control and PA-YK ($p < 0.05$) at both 4 and 24 h (Figure 2E, F). In contrast, the levels of all four genes were comparable between the control and PA-YK at both 4 and 24 h. These results demonstrate that the nanomatrix does not elicit an inflammatory response under static conditions, and the addition of NO to the nanomatrix may reduce inflammation.

3.3. Nanomatrix Attenuates Inflammatory Responses under Static Conditions. NO has been shown to decrease inflammation.[26−28] Therefore, we investigated whether our PA nanomatrix could attenuate a pre-existing inflammatory environment. We repeated the static adhesion assay with
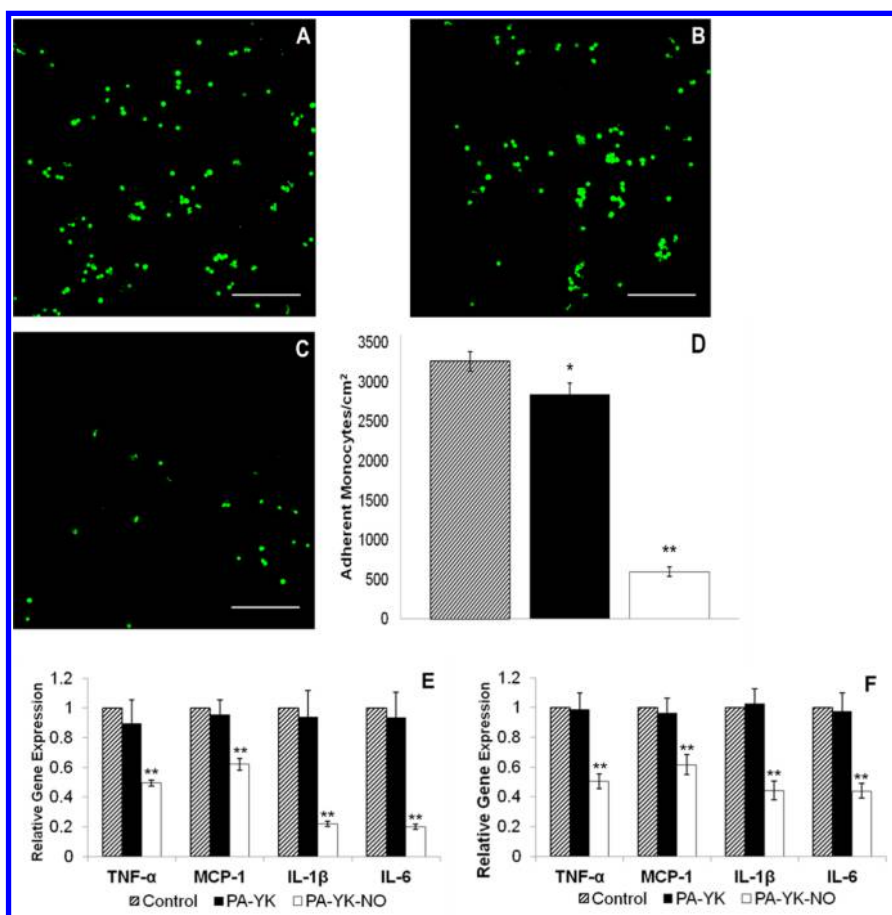
Figure 3. Static monocyte adhesion with TNF-α stimulation on HUVECs on (A) TCP control, (B) PA-YK, and (C) PA-YK-NO at 4 h. Scale bar = 300 μm. (D) Adherent monocyte quantification on TCP control, PA-YK, and PA-YK-NO at 4 h. (E, F) Relative gene expression of monocytes at (E) 4 and (F) 24 h. Bars show mean $\pm$ standard deviation. $*p < 0.01$. $**p < 0.001$.
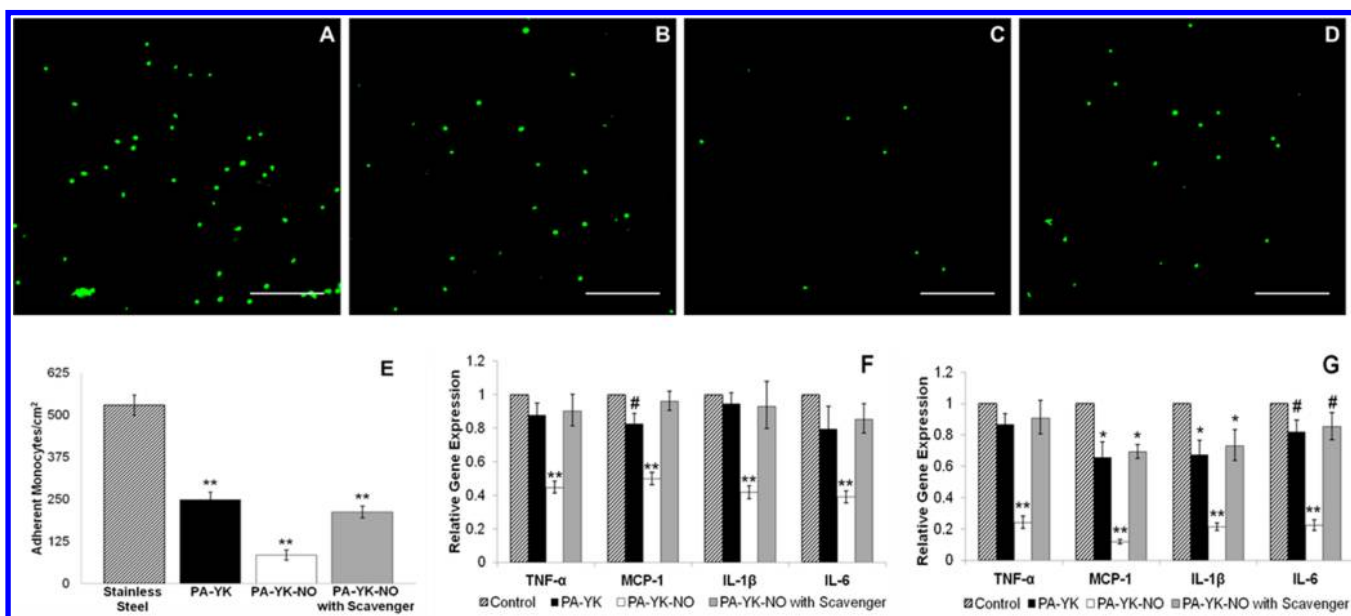

Figure 4. Monocyte adhesion under physiological flow on HUVECs on (A) stainless steel control, (B) PA-YK, (C) PA-YK-NO, and (D) PA-YK-NO with carboxy-PTIO at 4 h. Scale bar = 300 μm. (E) Adherent monocyte quantification on stainless steel control, PA-YK, PA-YK-NO, and PA-YK-NO with carboxy-PTIO at 4 h. (F, G) Relative gene expression of monocytes at (F) 4 and (G) 24 hours. Bars show mean $\pm$ standard deviation. $\#p < 0.05$. $*p < 0.01$. $**p < 0.001$.

TNF-α stimulation of the HUVECs, as TNF-α is known to increase endothelial cell expression of adhesive ligands for monocyte and leukocyte binding and contribute to endothelial dysfunction.[3] Figure 3 depicts monocyte adhesion on TNF-α
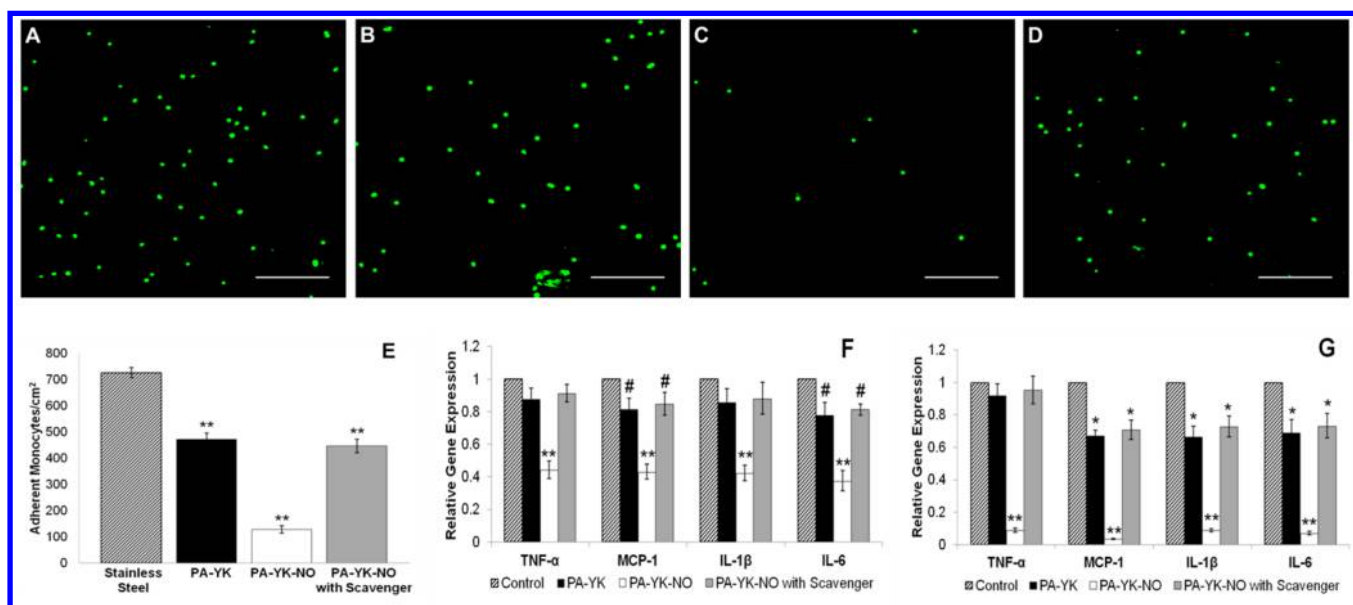
Figure 5. Monocyte adhesion under physiological flow with TNF-α stimulation on HUVECs on (A) stainless steel control, (B) PA-YK, (C) PA-YK-NO, and (D) PA-YK-NO with carboxy-PTIO at 4 h. Scale bar = 300 μm. (E) Adherent monocyte quantification on stainless steel control, PA-YK, PA-YK-NO, and PA-YK-NO with carboxy-PTIO at 4 h. (F, G) Relative gene expression of monocytes at (F) 4 and (G) 24 h. Bars show mean $\pm$ standard deviation. #$p < 0.05$. *$p < 0.01$. **$p < 0.001$.

stimulated HUVECs cultured on TCP, PA-YK, and PA-YK-NO. Monocyte adhesion was significantly reduced on TNF-α stimulated HUVECs cultured on PA-YK-NO (599 $\pm$ 59 cells/cm^2) compared to both TCP (3266 $\pm$ 124 cells/cm^2) and PA-YK (2847 $\pm$ 142 cells/cm^2) ($p < 0.001$) and as shown from both image (Figure 3A-C) and cell count (Figure 3D) data. Interestingly, monocyte adhesion to TNF-α stimulated HUVECs cultured on PA-YK was also slightly decreased compared to TCP controls, although not to the extent of PA-YK-NO (Figure 3A-D), suggesting that the nanomatrix alone may be of some benefit under inflammatory conditions. qRT-PCR analysis of the four monocyte inflammatory genes (TNF-α, MCP-1, IL-1β, and IL-6) revealed that PA-YK-NO was highly protective: all four monocyte inflammatory genes were significantly decreased ($p < 0.001$) compared to both TCP and PA-YK at both 4 and 24 h (Figure 3E, F). The gene expression levels between PA-YK and TCP, however, were comparable, suggesting that the NO was responsible for the anti-inflammatory effects. These results underline the protective effects of NO against inflammatory responses, reaffirming previous studies' findings.[26−28]

3.4. Nanomatrix Does Not Elicit an Inflammatory Response under Dynamic Flow in a Physiological Condition-Modeling Bioreactor. The promising results from the static studies prompted us to investigate the anti-inflammatory effects of our nanomatrix under dynamic flow within a physiological condition-modeling bioreactor. Stainless steel strips coated with PA-YK, PA-YK-NO, or left uncoated were utilized as the test surfaces within the bioreactor. We first investigated whether the nanomatrix might cause inflammatory responses under flow. Figure 4 shows monocyte adhesion to HUVECs cultured on bare, PA-YK, and PA-YK-NO coated stainless steel under arterial physiological flow rates of 10 dyn/cm^2.[30,31] Monocyte adhesion was significantly reduced on the HUVECs cultured on the PA-YK-NO coated stainless steel (84 $\pm$ 15 cells/cm^2) compared to both bare (529 $\pm$ 30 cells/cm^2) and PA-YK (249 $\pm$ 22 cells/cm^2) coated strips ($p < 0.001$) as

demonstrated by both image (Figure 4A-C) and cell count (Figure 4E) data. Monocyte adhesion to HUVECs cultured on PA-YK coated strips was also significantly reduced ($p < 0.001$) compared to bare stainless steel, and to a greater extent than that found under static conditions. This phenomenon may be due to the coating surface hardness compared to bare stainless steel. It has been shown that hard, rough surfaces such as modified titanium and stainless steel have increased monocyte and leukocyte adhesion compared to surfaces with more yield and lower surface roughness, such as multilayered fibrinogen and our nanomatrix coating.[33−35] Our previous studies have demonstrated that our nanomatrix coating forms a stable, smooth, uniform surface on stents; this may be a critical factor in prevention of inflammatory cell adhesion.[25] Thus, the nanomatrix coating itself may be protective under flow against inflammatory cell adhesion, although the addition of NO increased this protection. To investigate the effect of NO, the dynamic adhesion assay for PA-YK-NO-coated stainless steel was repeated with the addition of 100 μM carboxy-PTIO, a well-known NO scavenger.[36,37] Carboxy-PTIO reacts rapidly with NO to form predominantly nitrite; thus, it was used to scavenge and negate the therapeutic effect of the NO released by the coating.[36,37] In the presence of 100 μM carboxy-PTIO, monocyte adhesion to HUVECs cultured on PA-YK-NO (212 $\pm$ 18) was comparable to PA-YK (Figure 4B, D, E), suggesting that NO was indeed responsible for the significant decrease in monocyte adhesion. These results were further investigated by qRT-PCR of the four monocyte inflammatory genes examined during the static studies. PA-YK-NO significantly decreased the expression levels of all four inflammatory genes compared to both bare and PA-YK-coated stainless steel ($p < 0.001$) at both 4 and 24 h (Figure 4F, G). Gene expression on PA-YK samples was also decreased for some, but not all, of the monocyte inflammatory genes relative to the bare stainless steel, but not to the extent of PA-YK-NO. Addition of carboxy-PTIO to PA-YK-NO abolished the observed inflammatory gene reduction, returning gene expression to levels comparable to PA-YK, thus

exhibiting the impact of NO. Interestingly, the inflammatory gene expression levels decreased over time (4 to 24 h), which is in contrast to the trend under static conditions, which either remained stable or slightly increased between the 4 and 24 h time points. As with adhesion, it is possible that the nanomatrix coating with more yield is not as pro-inflammatory as the hard stainless steel surface, because it more closely mimics the native endothelial lumen of the cardiovascular vessel.[24,25] This could explain the decreased monocyte adhesion and inflammatory gene expression of the nanomatrix-coated surfaces. These results demonstrate that the nanomatrix does not cause an inflammatory response under dynamic flow conditions, and may in fact be protective. Furthermore, the results from PA-YK-NO demonstrate the ability of the coating to reduce inflammation under physiological flow, highlighting the importance of NO for inflammatory response reduction.

3.5. Nanomatrix Attenuates Inflammatory Responses under Dynamic Flow in a Physiological Condition-Modeling Bioreactor.
Because the nanomatrix demonstrated such promising results from the static studies and did not elicit inflammatory responses under dynamic flow, we repeated the flow studies with TNF-α stimulation. Figure 5 depicts monocyte adhesion to TNF-α stimulated HUVECs under physiological flow rates as described above. Again, monocyte adhesion was significantly reduced on TNF-α stimulated HUVECs cultured on PA-YK-NO coated stainless steel (127 $\pm$ 14 cells/cm^2) compared to both bare (727 $\pm$ 19 cells/cm^2) and PA-YK (472 $\pm$ 24 cells/cm^2)-coated strips ($p < 0.001$) as shown in both image (Figure 5A−C) and cell count (Figure 5E) data. Likewise, the addition of 100 μM carboxy-PTIO to HUVECs cultured on PA-YK-NO negated the effect of NO: monocyte adhesion (447 $\pm$ 26) was comparable to PA-YK (Figure 5B, D, and E). These results exhibit the protective effects of NO against inflammatory cell adhesion to endothelial cells, even in an inflammatory environment; this is a crucial consideration in stent coating design. Likewise, monocyte adhesion to TNF-α stimulated HUVECs cultured on PA-YK-coated strips was also significantly reduced ($p < 0.001$) compared to bare stainless steel, although not to the same extent as PA-YK-NO, demonstrating that the nanomatrix may be protective under flow in a pre-existing inflammatory environment. qRT-PCR further verified the trends discovered during the initial dynamic flow experiments: all four inflammatory gene expression levels were significantly decreased on PA-YK-NO compared to both bare and PA-YK coated stainless steel ($p < 0.001$) at both 4 and 24 h (Figure 5F, G), revealing the profound protective effects of NO against inflammatory responses. These findings were further investigated through immunocytochemical evaluation of the well-known NF-κB pro-inflammatory signaling and VCAM-1 adhesion molecule pathways. TNF-α stimulated HUVECs cultured on PA-YK coated strips exhibited nuclear translocation of NF-κB, thus exhibiting an inflamed state; in contrast, TNF-α stimulated HUVECs cultured on PA-YK-NO maintained diffuse NF-κB expression throughout the cells, indicative of a noninflammatory state (Figure 6A, B).

Likewise, TNF-α stimulated HUVECs cultured on PA-YK coated strips displayed higher VCAM-1 adhesion molecule expression compared to TNF-α stimulated HUVECs cultured on PA-YK-NO (Figure 6C, D). Taken together, the adhesion studies, qRT-PCR results, and immunocytochemistry demonstrate the ability of the endothelium-mimicking PA-YK-NO nanomatrix to reduce inflammation in a pre-existing inflamma-
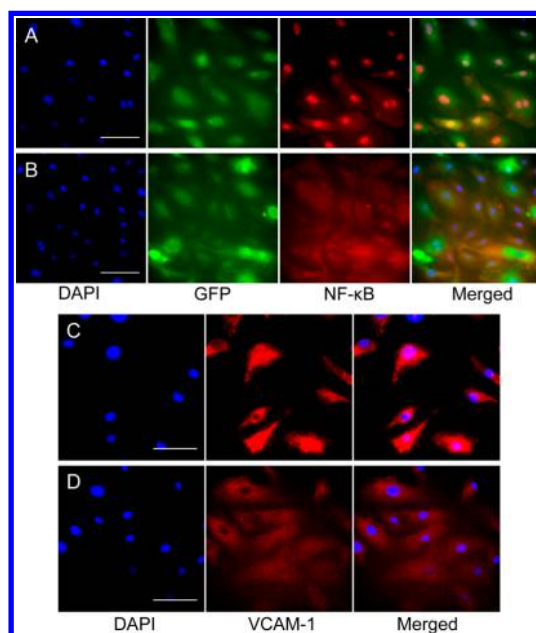

Figure 6. Immunocytochemistry under physiological flow with TNF-α stimulation on HUVECs. (A) NF-κB expression on PA-YK, (B) NF-κB expression on PA-YK-NO, (C) VCAM-1 expression on PA-YK, and (D) VCAM-1 expression on PA-YK-NO at 4 h. Scale bar = 100 μm.

tory environment under physiological flow conditions. Gene expression levels for PA-YK were decreased for some, but not all, of the monocyte inflammatory genes compared to bare stainless steel, but not nearly as much as PA-YK-NO. Furthermore, addition of carboxy-PTIO returned inflammatory gene expression to comparable levels to PA-YK, eliminating the anti-inflammatory effect of NO. These data corroborate previous studies, exhibiting the protective effects of NO against inflammation through both inflammatory cell adhesion and gene expression.[26−28] These results demonstrate that the nanomatrix can attenuate inflammatory responses under dynamic conditions, reducing both monocyte adhesion and inflammatory gene and molecule expression even in a pro-inflammatory environment induced by TNF-α. These experiments also underscore the importance of dynamic versus static experimentation for biological relevance, and the need for assays that more closely reflect physiology than inert environments for evaluation of biomedical implants.

3.6. Nanomatrix Successfully Dilates Vasoconstricted Rat Mesenteric Arterioles.
Since NO is well-known for its role as a vasodilator and in regulation of cardiovascular vessel diameter, we subsequently evaluated the bioavailability and bioactivity of the nanomatrix coating ex vivo in rat mesenteric arterioles (Figure 7A, B).[32,38−40] Following arteriole excision, cannulation, and stable constriction with phenylephrine, PA-YK-NO and PA-YK solutions were added directly to the vessel dilation chamber. As depicted in Figure 7G, PA-YK-NO instigated an immediate vasodilatory response, rapidly dilating the arteriole and increasing the diameter by up to 260% over its baseline constricted value (from 45 to 162 μm). This burst response subsequently tapered off, returning to baseline constricted values within 6 min of PA-YK-NO solution addition (Figure 7G). In contrast, PA-YK control did not elicit a vasodilatory response, which was expected since it did not contain NO. This experiment highlights the bioactivity of the
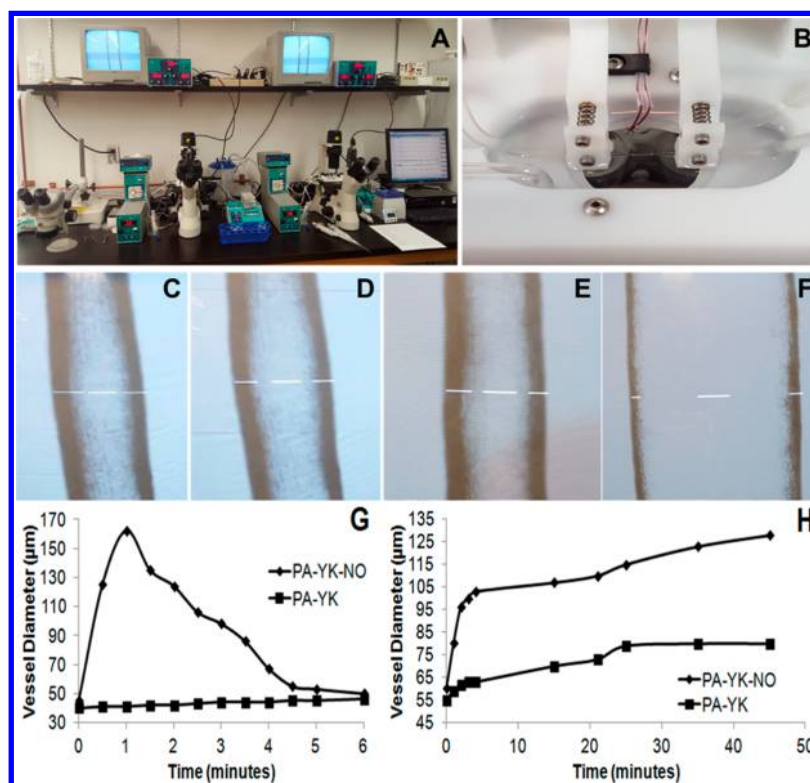
G

Figure 7. Ex vivo rat mesenteric arteriole vessel dilation. (A) Experimental setup. (B) Vessel in dilation camber. (C) PA-YK control added to vessel ($t = 0$). (D) Vessel with PA-YK control after 45 min. (E) PA-YK-NO added to vessel ($t = 0$). (F) Vessel with PA-YK-NO after 45 min. (G) PA-YK-NO and PA-YK solutions added to vessel dilation chamber. (H) PA-YK-NO- and PA-YK-coated 12 mm glass coverslips added to vessel dilation chamber.

NO released from the PA-YK-NO solution, but underscores the short-lived effect of a simple solution. When the PA-YK-NO and PA-YK were coated onto 12 mm glass coverslips, however, the sustained release kinetics of the nanomatrix were manifest. As expected, the PA-YK-coated control coverslip did not elicit a vasodilatory response (Figure 7C, D, and H). Conversely, the PA-YK-NO coated coverslip displayed an initial burst of NO followed by slow, sustained release from the nanomatrix over the duration of the experiment, which quickly dilated the arteriole and most notably maintained the dilated state, yielding an increase in diameter of 114% over its baselines constricted value (from 60 to 128 μm; Figure 7E, F, and H). This shows the highly desired release kinetics of NO from the PA-YK-NO nanomatrix, particularly as a stent coating: an initial burst release, followed by long, slow, sustained release over time. The immediate burst release is critical to arrest the initial neointimal hyperplasia and platelet adhesion following stent deployment, while the sustained release will maintain the nonproliferative state of the smooth muscle cells, antithrombogenicity of the vessel wall, and enhance endothelialization over the stent surface. The results of this ex vivo vasodilation study help to bridge the gap between cellular and whole tissue effects of the nanomatrix coating, validating the bioactivity of the coating prior to large-scale in vivo animal studies.

4. CONCLUSION

In the present study, we evaluated anti-inflammatory and vasodilatory effects of our endothelium-mimicking nanomatrix coating in vitro and ex vivo, respectively (Figures 1 and 7). Inflammation to implanted cardiovascular stents is a critical consideration in light of the adverse inflammatory responses to both bare metal and drug-eluting stents.[7−20] Therefore, we first investigated whether and to what extent the nanomatrix coating induced inflammation, and whether the nanomatrix coating could attenuate a pre-existing inflammatory environment. These experiments, performed under static conditions, indicated that the nanomatrix coating would be efficacious in both averting and attenuating inflammation. We next investigated the nanomatrix coating under dynamic physiological flow conditions, and found even more striking results: the nanomatrix coating both prevented and mitigated inflammatory responses, even within pre-existing inflammatory conditions; this was largely through the effects of NO, which could be blocked by addition of the NO scavenger. Finally, we demonstrated the bioavailability and bioactivity of our nanomatrix in an ex vivo rat mesenteric artery vasodilation experiment, exhibiting the ability of the NO-releasing nanomatrix coating to successfully dilate phenylephrine-constricted arterioles up to 114% over baseline constricted diameters, and manifesting desired NO release kinetics from PA-YK-NO for stent coatings. In addition to our previous work, these results indicate that this nanomatrix coating can address the clinical shortcomings of currently available DES, and paves the way for future studies in an appropriate in vivo animal model for cardiovascular stents.

■ AUTHOR INFORMATION

Corresponding Author
*E-mail: hwjun@uab.edu.

Notes

The authors declare no competing financial interest.

■ ACKNOWLEDGMENTS

■ REFERENCES

(1) Ross, R. The Pathogenesis of Atherosclerosis: A Perspective for the 1990s. *Nature* **1993**, *362*, 801−809.

(2) Perrins, C. J.; Bobryshev, Y. V. Current Advances in Understanding of Immunopathology of Atherosclerosis. *Virchows Arch.* **2011**, *458*, 117−123.

(3) Khan, R.; Spagnoli, V.; Tardif, J. C.; L'Allier, P. L. Novel Anti-Inflammatory Therapies for the Treatment of Atherosclerosis. *Atherosclerosis* **2015**, *240*, 497−509.

(4) Schaper, F.; Rose-John, S. Interleukin-6: Biology, Signaling and Strategies of Blockade. *Cytokine Growth Factor Rev.* **2015**, *26*, 475.

(5) Nakashima, Y.; Sun, D. H.; Trindade, M. C.; Chun, L. E.; Song, Y.; Goodman, S. B.; Schurman, D. J.; Maloney, W. J.; Smith, R. L. Induction of Macrophage C-C Chemokine Expression by Titanium Alloy and Bone Cement Particles. *J. Bone Jt. Surg., Br. Vol.* **1999**, *81*, 155−162.

(6) Melgarejo, E.; Medina, M. A.; Sanchez-Jimenez, F.; Urdiales, J. L. Monocyte Chemoattractant Protein-1: A Key Mediator in Inflammatory Processes. *Int. J. Biochem. Cell Biol.* **2009**, *41*, 998−1001.

(7) Joner, M.; Finn, A. V.; Farb, A.; Mont, E. K.; Kolodgie, F. D.; Ladich, E.; Kutys, R.; Skorija, K.; Gold, H. K.; Virmani, R. Pathology of Drug-Eluting Stents in Humans: Delayed Healing and Late Thrombotic Risk. *J. Am. Coll. Cardiol.* **2006**, *48*, 193−202.

(8) Finn, A. V.; Joner, M.; Nakazawa, G.; Kolodgie, F.; Newell, J.; John, M. C.; Gold, H. K.; Virmani, R. Pathological Correlates of Late Drug-Eluting Stent Thrombosis: Strut Coverage as a Marker of Endothelialization. *Circulation* **2007**, *115*, 2435−2441.

(9) Hwang, S. J.; Park, K. W.; Kwon, D. A.; Kang, H. J.; Koo, B. K.; Chae, I. H.; Gwon, H. C.; Park, S. J.; Seung, K. B.; Ahn, T.; Yoon, J. H.; Jang, Y. S.; Jeong, M. H.; Tahk, S. J.; Kim, H. S. Korea Stent Thrombosis, I. High Plasma Interleukin-6 Is Associated with Drug-Eluting Stent Thrombosis: Possible Role of Inflammatory Cytokines in the Development of Stent Thrombosis from the Korea Stent Thrombosis Registry. *Circ. J.* **2011**, *75*, 1350−1357.

(10) Shuchman, M. Trading Restenosis for Thrombosis? New Questions About Drug-Eluting Stents. *N. Engl. J. Med.* **2006**, *355*, 1949−1952.

(11) Farb, A.; Sangiorgi, G.; Carter, A. J.; Walley, V. M.; Edwards, W. D.; Schwartz, R. S.; Virmani, R. Pathology of Acute and Chronic Coronary Stenting in Humans. *Circulation* **1999**, *99*, 44−52.

(12) Gogo, P. B., Jr.; Schneider, D. J.; Watkins, M. W.; Terrien, E. F.; Sobel, B. E.; Dauerman, H. L. Systemic Inflammation after Drug-Eluting Stent Placement. *J. Thromb. Thrombolysis* **2005**, *19*, 87−92.

(13) Kang, W. C.; Ahn, T. H.; Moon, C. I.; Han, S. H.; Shin, E. K.; Kim, J. S.; Ko, Y. G.; Choi, D.; Jang, Y.; Kim, B. K.; Oh, S. J.; Jeon, D. W.; Yang, J. Y. Comparison of Inflammatory Markers and Angiographic Outcomes after Implantation of Sirolimus and Paclitaxel-Eluting Stents. *Heart* **2009**, *95*, 970−975.

(14) Li, J. J.; Qin, X. W.; Yang, X. C.; Li, Z. C.; Zeng, H. S.; Xu, B.; Gao, Z.; Wu, Y. J.; Zhang, X.; Zhang, C. Y. Randomized Comparison of Early Inflammatory Response after Sirolimus-Eluting Stent Vs Bare Metal Stent Implantation in Native Coronary Lesions. *Clin. Chim. Acta* **2008**, *396*, 38−42.

(15) Li, J. J.; Yan, H. B.; Xiang, X. P.; Qin, X. W.; Zhang, C. Y. Comparison of Changes in Early Inflammatory Markers between Sirolimus- and Paclitaxel-Eluting Stent Implantation. *Cardiovasc. Drugs Ther.* **2009**, *23*, 137−143.

(16) Wilson, G. J.; Nakazawa, G.; Schwartz, R. S.; Huibregtse, B.; Poff, B.; Herbst, T. J.; Baim, D. S.; Virmani, R. Comparison of Inflammatory Response after Implantation of Sirolimus- and Paclitaxel-Eluting Stents in Porcine Coronary Arteries. *Circulation* **2009**, *120*, 141−149.

(17) Wood, S. C.; Tang, X.; Tesfamariam, B. Paclitaxel Potentiates Inflammatory Cytokine-Induced Prothrombotic Molecules in Endothelial Cells. *J. Cardiovasc. Pharmacol.* **2010**, *55*, 276−285.

(18) Sambu, N.; Dent, H.; Englyst, N.; Warner, T. D.; Leadbeater, P.; Roderick, P.; Gray, H.; Simpson, I.; Corbett, S.; Calver, A.; Morgan, J.; Curzen, N. Effect of Clopidogrel Withdrawal on Platelet Reactivity and Vascular Inflammatory Biomarkers 1 Year after Drug-Eluting Stent Implantation: Results of the Prospective, Single-Centre Cessation Study. *Heart* **2011**, *97*, 1661−1667.

(19) Wu, Y.; Zhang, W.; Liu, W.; Zhuo, X.; Zhao, Z.; Yuan, Z. The Double-Faced Metabolic and Inflammatory Effects of Standard Drug Therapy in Patients after Percutaneous Treatment with Drug-Eluting Stent. *Atherosclerosis* **2011**, *215*, 170−175.

(20) Joner, M.; Nakazawa, G.; Finn, A. V.; Quee, S. C.; Coleman, L.; Acampado, E.; Wilson, P. S.; Skorija, K.; Cheng, Q.; Xu, X.; Gold, H. K.; Kolodgie, F. D.; Virmani, R. Endothelial Cell Recovery between Comparator Polymer-Based Drug-Eluting Stents. *J. Am. Coll. Cardiol.* **2008**, *52*, 333−342.

(21) Puskas, J. E.; Munoz-Robledo, L. G.; Hoerr, R. A.; Foley, J.; Schmidt, S. P.; Evancho-Chapman, M.; Dong, J.; Frethem, C.; Haugstad, G. Drug-Eluting Stent Coatings. *Wiley Interdiscip. Rev.: Nanomed. Nanobiotechnol.* **2009**, *1*, 451−462.

(22) Kushwaha, M.; Anderson, J. M.; Bosworth, C. A.; Andukuri, A.; Minor, W. P.; Lancaster, J. R., Jr.; Anderson, P. G.; Brott, B. C.; Jun, H. W. A Nitric Oxide Releasing, Self Assembled Peptide Amphiphile Matrix That Mimics Native Endothelium for Coating Implantable Cardiovascular Devices. *Biomaterials* **2010**, *31*, 1502−1508.

(23) Andukuri, A.; Minor, W.; Kushwaha, M.; Anderson, J.; Jun, H. W. Effect of Endothelium Mimicking Self-Assembled Nanomatrices on Cell Adhesion and Spreading of Human Endothelial Cells and Smooth Muscle Cells. *Nanomedicine* **2010**, *6*, 289−297.

(24) Andukuri, A.; Sohn, Y.; Anakwenze, C.; Lim, D.; Brott, B.; Yoon, Y.; Jun, H. Enhanced Human Endothelial Progenitor Cell Adhesion and Differentiation by a Bioinspired Multifunctional Nanomatrix. *Tissue Eng., Part C* **2013**, *19*, 375−385.

(25) Andukuri, A.; Min, I.; Hwang, P.; Alexander, G.; Marshall, L. E.; Berry, J. L.; Wick, T. M.; Joung, Y. K.; Yoon, Y. S.; Brott, B. C.; Han, D. K.; Jun, H. W. Evaluation of the Effect of Expansion and Shear Stress on a Self-Assembled Endothelium Mimicking Nanomatrix Coating for Drug Eluting Stents in Vitro and in Vivo. *Biofabrication* **2014**, *6*, 035019.

(26) Kubes, P.; Suzuki, M.; Granger, D. N. Nitric Oxide: An Endogenous Modulator of Leukocyte Adhesion. *Proc. Natl. Acad. Sci. U. S. A.* **1991**, *88*, 4651−4655.

(27) Harrison, C. B.; Drummond, G. R.; Sobey, C. G.; Selemidis, S. Evidence That Nitric Oxide Inhibits Vascular Inflammation and Superoxide Production Via a P47phox-Dependent Mechanism in Mice. *Clin. Exp. Pharmacol. Physiol.* **2010**, *37*, 429−434.

(28) Lavin, B.; Gomez, M.; Pello, O. M.; Castejon, B.; Piedras, M. J.; Saura, M.; Zaragoza, C. Nitric Oxide Prevents Aortic Neointimal Hyperplasia by Controlling Macrophage Polarization. *Arterioscler., Thromb., Vasc. Biol.* **2014**, *34*, 1739−1746.

(29) Walmet, P. S.; Eckman, J. R.; Wick, T. M. Inflammatory Mediators Promote Strong Sickle Cell Adherence to Endothelium under Venular Flow Conditions. *Am. J. Hematol.* **2003**, *73*, 215−224.

(30) Dammers, R.; Stifft, F.; Tordoir, J.; Hameleers, J.; Hoeks, A.; Kitslaar, P. Shear Stress Depends on Vascular Territory: Comparison

between Common Carotid and Brachial Artery. *J. Appl. Physiol.* **2003**, *94*, 485−489.

(31) Sheikh, S.; Rainger, G.; Gale, Z.; Rahman, M.; Nash, G. Exposure to Fluid Shear Stress Modulates the Ability of Endothelial Cells to Recruit Neutrophils in Response to Tumor Necrosis Factor-Alpha: A Basis for Local Variations in Vascular Sensitivity to Inflammation. *Blood* **2003**, *102*, 2828−2834.

(32) Jang, H. J.; Ridgeway, S. D.; Kim, J. A. Effects of the Green Tea Polyphenol Epigallocatechin-3-Gallate on High-Fat Diet-Induced Insulin Resistance and Endothelial Dysfunction. *Am. J. Physiol.: Endocrinol. Metab.* **2013**, *305*, E1444−1451.

(33) Goransson, A.; Gretzer, C.; Johansson, A.; Sul, Y. T.; Wennerberg, A. Inflammatory Response to a Titanium Surface with Potential Bioactive Properties: An in Vitro Study. *Clin. Implant Dent. Relat. Res.* **2006**, *8*, 210−217.

(34) Schuler, P.; Assefa, D.; Ylanne, J.; Basler, N.; Olschewski, M.; Ahrens, I.; Nordt, T.; Bode, C.; Peter, K. Adhesion of Monocytes to Medical Steel as Used for Vascular Stents Is Mediated by the Integrin Receptor Mac-1 (Cd11b/Cd18; Alpham Beta2) and Can Be Inhibited by Semiconductor Coating. *Cell Commun. Adhes.* **2003**, *10*, 17−26.

(35) Safiullin, R.; Christenson, W.; Owaynat, H.; Yermolenko, I. S.; Kadirov, M. K.; Ros, R.; Ugarova, T. P. Fibrinogen Matrix Deposited on the Surface of Biomaterials Acts as a Natural Anti-Adhesive Coating. *Biomaterials* **2015**, *67*, 151−159.

(36) Akaike, T.; Yoshida, M.; Miyamoto, Y.; Sato, K.; Kohno, M.; Sasamoto, K.; Miyazaki, K.; Ueda, S.; Maeda, H. Antagonistic Action of Imidazolineoxyl N-Oxides against Endothelium-Derived Relaxing Factor/.No through a Radical Reaction. *Biochemistry* **1993**, *32*, 827−832.

(37) Pfeiffer, S.; Leopold, E.; Hemmens, B.; Schmidt, K.; Werner, E. R.; Mayer, B. Interference of Carboxy-Ptio with Nitric Oxide- and Peroxynitrite-Mediated Reactions. *Free Radical Biol. Med.* **1997**, *22*, 787−794.

(38) Furchgott, R. F.; Zawadzki, J. V. The Obligatory Role of Endothelial Cells in the Relaxation of Arterial Smooth Muscle by Acetylcholine. *Nature* **1980**, *288*, 373−376.

(39) Nathan, C. Nitric Oxide as a Secretory Product of Mammalian Cells. *FASEB J.* **1992**, *6*, 3051−3064.

(40) Kuo, P. C.; Schroeder, R. A. The Emerging Multifaceted Roles of Nitric Oxide. *Ann. Surg.* **1995**, *221*, 220−235.

(41) Rozen, S.; Skaletsky, H. J. *Primer3*, 1998; code available at http://www-genome.wi.mit.edu/genome_software/other/primer3.html.